Vol. 24, No. 2(2025) IA25505
Revista Mexicana de Ingeniería Química

Enhancement of rheological and filtration properties of water-based drilling fluids through zinc oxide nanoparticles addition

Mejoramiento de las propiedades reológicas y de filtración de un fluido de perforación base agua mediante la adición de nanopartículas de óxido de zinc

L.C. Rodríguez-López[1], H. Pérez-Vidal[1], F.C. Gómez-Torres[2], C. Martínez-Pacheco[2], E.E. Uicab-Córdova[3], S.C. Madrigal-Díaz[4], L.L. Díaz-Flores[4]*
[1]Academic Division of Basic Sciences, Juarez Autonomous University of Tabasco, Tabasco, México.
[2]Division of Industrial Process, Technological University of Tabasco, Tabasco, México.
[3]Division of Chemistry, Technological University of Tabasco, Tabasco, México.
[4]Academic Division of Engineering and Architecture, Juarez Autonomous University of Tabasco, Tabasco, México.
Received: January 17, 2025; Accepted: April 12, 2025

Abstract
Drilling fluids are used in oil well drilling depending on their filtration characteristics and rheological properties. Because of the increase in environmental policies, innovations in water-based drilling fluids (WBDF) have been proposed to convert them into high-performance fluids with stabilizer properties during drilling, avoiding an increase in non-productive time (NPT) and costs. This study proposes the enhancement of WBDF due to the addition of ZnO nanoparticles (ZnO-NPs). After the addition of ZnO-NPs, the results show that the drilling fluid, with a concentration of 0.05 % ZnO-NPs, has improved rheological properties, evaluated at 25, 50, and 70 °C. At room temperature, there is an increase in other parameters such as apparent viscosity (AV) 200 %, the plastic viscosity (PV) 180 %, the yield point (YP) 240 %, compared to the base fluid and furthermore 10-min gel strength elevates by 80 % more. In addition, the amount of filtered fluid reduces from 13.5 to 10.4 mL, even under conditions of 500 psi and 150 °C, there is a 54 % reduction, indicating the formation of a proper filter cake.
Keywords: Filtration control, HPHT conditions, Mechanosynthesis, ZnO nanoparticles, Water-based drilling fluids.

Resumen
Los fluidos de perforación se utilizan en la perforación de pozos petroleros dependiendo de sus características de filtración y propiedades reológicas. Debido al aumento de las políticas ambientales, se han propuesto innovaciones en los fluidos de perforación a base de agua (WBDF) para convertirlos en fluidos de alto rendimiento con propiedades estabilizadoras durante la perforación, evitando un aumento en el tiempo no productivo (NPT) y los costos. Este estudio propone el mejoramiento del WBDF debido a la adición de nanopartículas de ZnO (ZnO-NPs). Después de la adición de las ZnO-NPs, los resultados muestran que el fluido de perforación, con una concentración de 0.05% de ZnO-NPs, tiene propiedades reológicas mejoradas, evaluadas a 25, 50 y 70 °C. A temperatura ambiente, hay un aumento en otros parámetros como la viscosidad aparente (AV) 200 %, la viscosidad plástica (PV) 180 %, el límite elástico (YP) 240 %, en comparación con el fluido base y, además, la fuerza del gel de 10 minutos se eleva en un 80 % más. Además, la cantidad de fluido filtrado se reduce de 13,5 a 10,4 mL, incluso bajo condiciones de 500 psi y 150 °C, hay una reducción del 54%, lo que indica la formación de una torta de filtración adecuada.
Palabras clave: Control de filtración, condiciones HPHT, Mecanosíntesis, Nanopartículas de ZnO, Fluidos de perforación a base de agua.

*Corresponding author. *E-mail*: laura.diaz@ujat.mx ;
https://doi.org/10.24275/rmiq/IA25505
ISSN:1665-2738, *issn-e*: 2395-8472

1 Introduction

The petroleum industry contributes to the energy context due to global oil consumption, increasing since the beginning of this millennium, showing an upward production trend from 3,300 to 4,500 million tons of oil equivalent (toe) (Zheng *et al*., 2022). The growing energy demand and the continuous depletion of conventional oil reserves (Chuck H. *et al*., 2011) have compelled the energy sector to innovate existing technology to locate and drill complex formations (Nwaezeapu *et al*., 2019). Drilling is a decisive process for recovering underground materials such as oil and gas, and drilling fluids are key to achieving this goal (Sadeghalvaad & Sabbaghi, 2015). Furthermore, these fluids are used to suspend cuttings, clean the wellbore (Ofei *et al*., 2021), cool the drill (Yi *et al*., 2024), preserve effective lubrication between the drilling equipment and the well (Lysakova *et al*., 2024), conserve proper weight-on-bit pressure (Reilly *et al*., 2016), and provide wellbore stability (Ma *et al*., 2024). The success of a drilling operation depends on the fluid's composition and properties of the drilling (Aghdam et al., 2020). On the other hand, the selection and quantity of additives in drilling fluids affect the rheology and the desired filtration properties of the fluid (Al-Zubaidi *et al*., 2017). An incorrect formulation of the fluid generates problems during the drilling process, particularly filtrate loss across the formation, resulting in an excessively thick filter cake (Y. Duan *et al*., 2024). This infiltration of the liquid and solid phase of the drilling mud in the reservoir formation affects the hydrocarbon production rate and the liquid phase of the drilling mud could create water-in-oil emulsion (w/o). These problems are avoided when enhancing filtration properties by decreasing the amount of lost volume of the drilling fluid, and by rising rheological properties, such as elastic limit, gel strength and shear rate, drilling mud performance is improved (Ghayedi & Khosravi, 2020). Highly efficient drilling fluids are essential for drilling in challenging zones, such as high-pressure, high-temperature (HPHT) formations (Sulaimon *et al*., 2017).

With recent progress in nanotechnology, Ibrahim *et al*. (2024), Yi *et al*. (2024), and Oseh *et al*. (2024) have studied the possibility of using nanoparticles (NPs) and their integration with natural and synthetic polymers in the petroleum industry. This is because nanomaterials have specific characteristics of surface effect and small-size (Friedheim et al., 2012). These features make them suitable as additives to modify the rheology and filtration properties of WBDF (Rafati *et al*., 2018).

In relation to this topic, Pourkhalil H. and Nakhaee, A. (2019), report the use of different nanoparticles as additives in drilling fluids; they used three Nano-ZnO fluids with different concentrations. These fluids caused a reduction in pore pressure accumulation and proved a desirable effect in blocking pore spaces in the shale samples.

Studies conducted by Ahmad *et al*., (2021), showed the synergistic effect of the polymer and nanoparticles on the hydration of shale and the swelling performance of drilling fluids, confirming that it enhances the inhibition characteristics.

A study of the thermal stability of the fluid, by Medhi *et al*., (2021), found that the addition of ZnO-NP in the water-based drilling nanofluid increase viscosity and reduce fluid loss.

Currently, the formulation of drilling mud has been studied to lower costs, and to reduce the damage caused by the filtration of the mud due to its inefficient stability at high temperatures and pressures (Martin *et al*., 2024), in addition to preserving the environment, without compromising the performance of the fluid and its functions (Ramos et al., 2013).

Therefore, the main objective of this work was to investigate the effect of the addition of ZnO-NPs synthesized by mechanochemical synthesis and incorporating different concentrations to WBDF, to evaluate the behavior of its rheological and filtration properties. In this study it was demonstrated that with short milling times of the inorganic precursors for obtaining ZnO nanoparticles, it is possible to obtain characteristics that contribute to improving the rheological and filtration properties of a WBDF formulation using bentonite and chemical additives.

2 Materials and methods

2.1 Synthesis of ZnO-NPs

Mechanosynthesis method was used to synthesize ZnO, applying as precursors: 3.45 g of J.T. Baker zinc chloride ($ZnCl_2$) at 97% purity, 2.62 g of J.T. Baker sodium carbonate (Na_2CO_3) at 99.5% purity and 11.48 g of sodium chloride (NaCl) or common table salt. These precursors were mixed in a 92.87 mL stainless steel container with stainless steel milling media, which was grinded in a 60 Hz mill (8000M millSpex@), at different milling times: 20, 40 and 60 min, samples were named ZnO 20, ZnO 40 and ZnO 60. The grinding time used to obtain ZnO-NPs was taken from literature reports. (Espitia *et al*., 2012; Sapkota *et al*., 2021), due to its influence on the physical and chemical properties of the nanoparticles. As grinding time increases, the particles tend to reduce their size due to continuous fracture and cold welding, resulting in a higher specific surface area (Abrica G. and Gómez A., 2022). Furthermore, grinding time induce transformations in the crystalline structure of

materials, even long grinding times can lead to the nanoparticles being contaminated by materials from the milling media (such as the grinding balls and the vial), which negatively affect the final material properties (Prieto G. *et al*., 2007).

After milling, the ZnO was separated from the NaCl residue derived from the reaction, with three washing processes with distilled water and vacuum filtration, then ultrasound treatment was conducted for 60 min and washed one more time. Subsequently, the sample was dried in the oven at 120 °C for 2 h and then calcined at 400 °C for 2 h with a ramp rate of 10 °C/min. 3 types of nanoparticles were obtained, labeled depending on the time as ZnO X, where X= 20, 40 and 60.

2.2 *Characterization of ZnO-NPs*

X-ray Diffraction (XRD) was conducted for the analysis of the crystalline phase obtained and the crystal size of the ZnO powders, using an x-ray diffractometer (Bruker D8-Advance) having a CuKα1 radiation with a wavelength of λ=1.54060 Å, 40 Kv and 30 mA. The intensity of the peaks was measured in a range of 20° to 80° in 2θ.

RAMAN spectroscopy was used to identify the structure of the Zn-O bonds, with a WITEC Alpha 300 spectrometer measuring from 50 to 700 cm^{-1}, the laser wavelength was 488 nm, with an integration time of 1s. The ZnO powders were also analyzed by FTIR spectroscopy Shimadzu IRAffinity-1 spectrometer, in the range of 4700 to 370 cm^{-1}.

The morphology of the ZnO powders was determined by Field Emission Scanning Electron Microscopy (FESEM). A JEOL JSM-7600F microscope was employed at 15 kV acceleration voltage, with a field emission gun, with a secondary electron detector.

Particle Size Distribution and Dynamic Light Scattering were carried out Zeta sizer equippment Malvern Panalytical^{TM} model ZS, in solutions at a concentration of 5 mg of material in 10 mL of dispersant in polystyrene disposable cell using Stokes Einstein equation. These techniques were used to characterize stability and surface distribution of ZnO-NPs Water-Based Drilling Fluid.

Finally, the specific area was measured in a Micromeritics^{TM} model TriStar II 320 low-pressure nitrogen adsorption analysis equipment, using the BET method (Brunauer, Emmett and Teller).

2.3 *Preparation of the Water-Based Drilling Fluid (WBDF)*

To compare the effect of the addition of the ZnO-NPs into the fluid, a WBDF, called base fluid, was prepared, mixing sodium bentonite treated with water at 10 % w/v, this mixture was left for 24 h for hydration, and water was added later until an apparent viscosity of 5 cP was obtained. Additives listed in Table 1 were also added. The resulting mixture was stirred at high-speed using a mechanical agitator, considering stirring for 30 min for each additive incorporated. Sonication was performed for 1 h for fluid homogenization.

Table 1. Additives used for the preparation of water-based drilling fluid.

Additives	% w/v
Bentonite ($Al_2O_3 \cdot 4SiO_2 \cdot H_2O$)	10.00
Xanthan gum (($C_{35}H_{49}O_{29}$)n)	0.25
Polyanionic cellulose ([$C_6H_7O_2(OH)_2CH_2COONa$]n)	0.50
Potassium chloride (KCl)	3.00
Sodium hydroxide (NaOH)	0.01
Formaldehyde (H_2C=O)	0.10

2.4 *Preparation of the modified water-based drilling fluid*

In order to evaluate the effect of ZnO-NPs on the rheological and filtration behavior of WBDF formulation, the modified water-based drilling fluid (MWBDF) was prepared. First, it began a coupling fluid called CF_1, CF_2 and CF_3 (according to the percentage of ZnO-NPs added) was obtained, in 200 mL of a mixture of bentonite with water, diluted to reach 5 cP, xanthan gum was incorporated at 0.25 % w/v stirring for 30 minutes. Afterwards, the synthesized ZnO-NPs were added at 20, 40 and 60 milling minutes, at a concentration of 0.05, 0.10 and 0.15 % w/v (Table 2), concentrations ≥ 0.20 % are not recomended due undesirable effects on water-based drilling fluids (Cardenas A., 2022). These fluids (CF_1, CF_2 and CF_3) were mechanically mixed for 30 min with the WBDF to obtain the MWBDF formulations.

Table 2. Coupling fluids (CF) for the preparation of a modified WBDF.

Nomenclature	% w/v of ZnO-NPs	% w/v of GX
CF_1	0.05	0.25
CF_2	0.10	0.25
CF_3	0.15	0.25

2.5 *Effect of ZnO-NPs on the rheological and filtration properties of water-based drilling fluid*

Each of the samples obtained from the WBDF was evaluated for its rheological and filtration properties. Triplicate tests were carried out, following the procedure and specifications recommended by the American Petroleum Institute (API) (API, 2019), using the appropriate equipment.

2.5.1 Evaluation of rheological properties

The rheological tests of the WBDF and the MWBDF with ZnO-NPs, were carried out with a Fann-35A viscometer; according to the API 13B-1 standard, these tests were tried at temperatures of 25, 50 and 70 °C and readings were recorded at 3, 6, 100, 200, 300 and 600 RPM, to make the measurements, the freshly stirred sample was placed inside a thermal vessel and heated to the test temperature.

2.5.1.1 Apparent viscosity

To calculate the VA, once the temperature was reached, the engine was started by placing the commutator in the high-speed position, with the speed shift lever in the lowest position and when the value was constant the reading at 600 RPM was recorded.

$$\text{Apparent viscosity, cP} = \frac{\text{reading for 600 RPM}}{2}$$

2.5.1.2 Viscosity plastic

To calculate PV, the switch was set to the speed of 300 RPM, when it indicated a constant value, the reading was taken for 300 RPM.

$$\text{Plastic viscosity, cP} = \text{reading at 600 RPM} - \text{reading at 300 RPM}$$

2.5.1.3 Yield point

For the calculation of the yield point, the formula was used:

$$\text{Yield point, lb/100 ft}^2 = \text{reading for 300 RPM} - \text{plastic viscosity}$$

2.5.1.4 Gel strength

For the measurement of the gel strength of 10 seconds and 10 minutes, the sample was stirred at 600 RPM, approximately 15 seconds and the velocity assembly were positioned in neutral; after that time, the engine was shut down, keeping the drilling fluid static for 10 seconds and 10 minutes, respectively. Subsequently, the switch was changed to a low-speed position and the maximum deflection units at 3 rpm were recorded. These readings are taken as values that represent gel strength.

2.5.2 Evaluation of filtration properties

Low-pressure and low-temperature filtration was measured for all samples of the MWBDF and WBDF using an OFITE low-pressure filter press at a pressure of 100 psi and room temperature (API 13B-1, 2019). The volume of fluid passing through the standard filter paper was recorded during 30 minutes within 5-minute intervals.

High-pressure and high-temperature (HPHT) filtration properties were measured at 500 psi and 150 °C using an OFITE HPHT filter press. The test was conducted for 30 minutes, and later the filtered fluid was collected and measured.

2.5.3 Hot-rolling process

400 mL samples of each formulation (WBDF and MWBDF) were poured into cylindrical aging cells and pressurized at 200 psi using CO_2 capsules, maintaining rotation inside the roller oven for 16 hours at 110 °C.

3 Results and discussion

3.1 Characterization of ZnO-NPs added to the WBDF formulation

The ZnO-NPs with milling times of 20, 40 and 60 minutes were analyzed by structural, morphological and textural techniques.

3.1.1 X-ray diffraction

The diffractograms presented in Figure 1 correspond to ZnO-NPs synthesized at three milling duration time: 20, 40, and 60 minutes. No significant differences were observed in the signal of the diffracted peaks, mainly on the (100), (002), and (101) planes. This confirms the successful synthesis of pure and crystalline particles. X-ray diffraction (XRD) analysis also showed the characteristic peaks of a hexagonal wurtzite crystal system, with lattice parameters of a=3.25 Å, b=3.25 Å and c=5.21 Å (Bolarinwa *et al.*, 2017). These results indicate that mechanochemical synthesis produces the crystal structure, consistent with the standard reference card (JCDPS: 00-036-1451).

The most intense peaks were observed at angles of 36.2° and 31.7°, corresponding to the (100) and (101) planes, respectively. Using the Debye–Scherrer equation, the calculated crystal sizes were in the ranges of 42 and 47 nm for ZnO 20; 45 and 48 nm for ZnO 40; and 42 and 47 nm for ZnO 60, corresponding to the main peaks mentioned above.

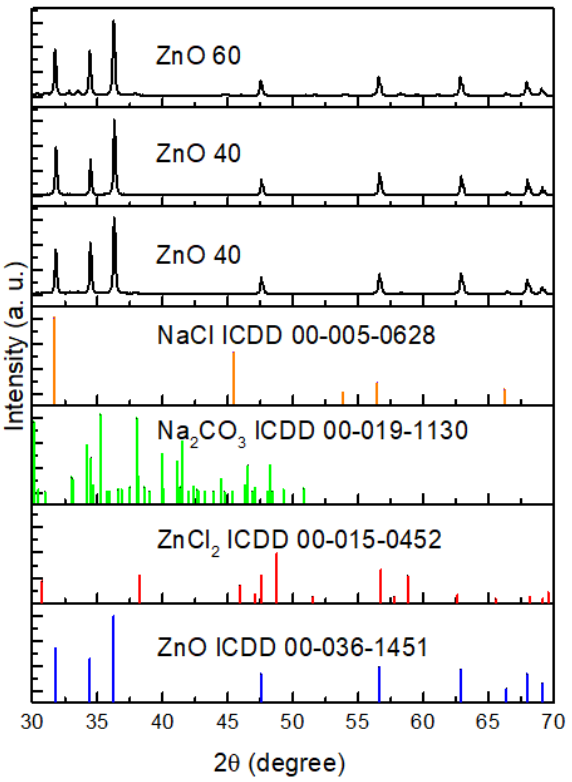

Figure 1. X-ray diffraction patterns of precursors and ZnO powders synthesized by mechanochemical route with varying grinding times of 20 (ZnO 20), 40 (ZnO 40), and 60 (ZnO 60) minutes, and synthesized at 450 °C.

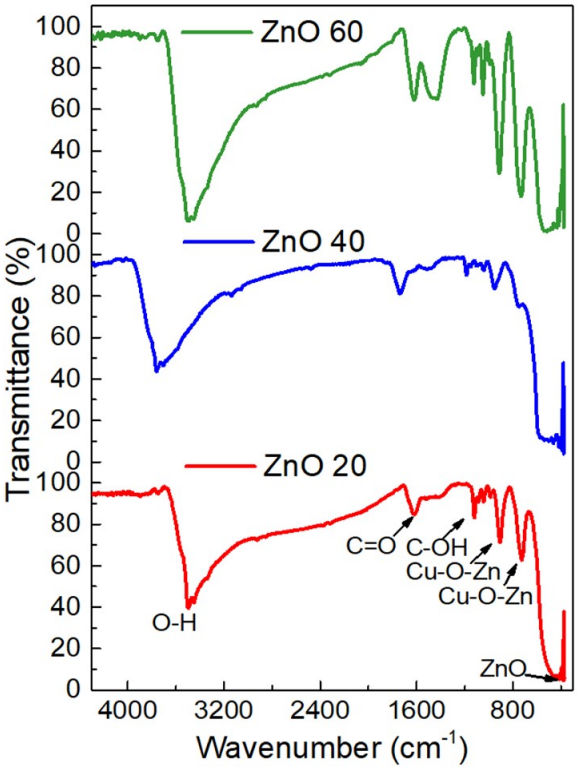

Figure 2. Fourier Transform Infrared (FTIR) spectra of ZnO powders synthesized via mechanochemical route with grinding times of 20, 40, and 60 minutes.

3.1.2 FTIR spectroscopy

As ZnO crystals were obtained by milling techniques, ZnO-NPs powders were analyzed to evaluate the presence of contaminants or residuals from the mechanochemical reaction. Figure 2 presents the FTIR spectra corresponding to the three milling samples. Distinct bands are observed in all three spectra: the band at 3500 cm^{-1} corresponds to the O-H functional group (hydroxyl groups), caused by both molecular and dissociative water absorption, resulting from the synthesis process and moisture absorption from the air (Aquino *et al*., 2018). The band at 1624 cm^{-1} and 1121 cm^{-1} is associated with the C=O functional group linked to symmetric stretching of sodium carbonate, and to the C-OH group resulting from bending, respectively (Senthilkumaar *et al*., 2008). The band at 902 cm^{-1} is associated with the formation of Zn with tetrahedral coordination (García M. *et al*., 2024) and the band at 720 cm^{-1} are attributed to Zn-O stretching (Zargar *et al*., 2014). Additionally, the band located at 380 cm^{-1} corresponds to the ZnO vibration (Aquino *et al*., 2018).

These spectra indicate that the ZnO-NPs samples at 60 min contain the highest amount of reaction residuals, which could potentially influence the rheological properties of the MWBDF formulated in this study.

3.1.3 Raman spectroscopy

Since the bands associated with the precursors appear in the FTIR analysis, the ZnO powders were analyzed by Raman spectroscopy. The peak observed at 100 cm^{-1} in Figure 3 belongs to the low-frequency mode of E_{2L}, related to the vibration of the Zn-sublattice; the peak at 333 cm^{-1} is an E_{2H}-E_{2L} vibrational mode developing from phonons of the boundary zone of wurtzite ZnO. The peak presented at 438 cm^{-1} corresponds to the high-frequency E_{2H} mode; this vibration mode occurs after the movement of oxygen atoms in the ZnO lattice (Tichaona Taziwa *et al*., 2017). Finally, the peak located at 580 cm^{-1} is E_1(LO) mode and originates from oxygen vacancy defects in ZnO (Qi *et al*., 2008). All samples present four vibrational modes characteristic of ZnO, sustaining the obtention of crystalline ZnO, which was observed in the diffractogram in Figure 1. The shift in spectral bands observed around 330 cm^{-1} and 430 cm^{-1} with different grinding times ocurrs due to temperature changes caused by mechanical action (Michael J. Pelletier, 1989) and the stress within the material by grinding time increase, affecting molecular vibrations (Ibáñez *et al*., 2023).

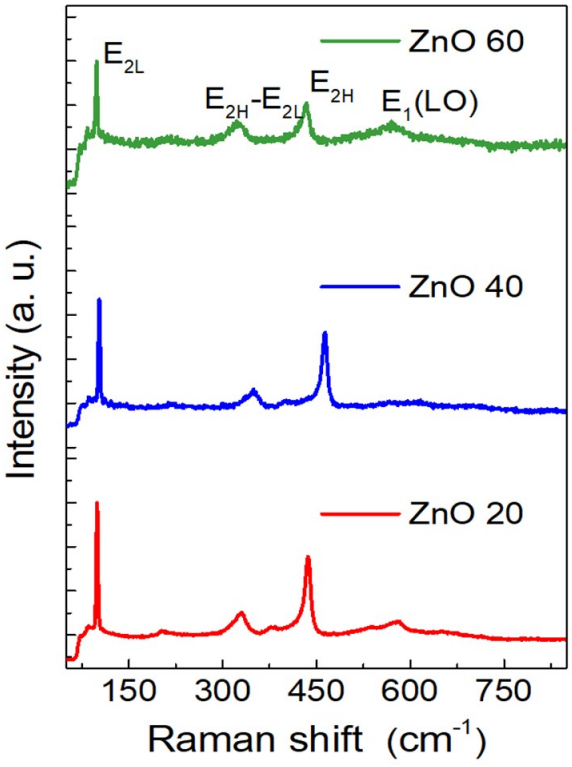

Figure 3. Raman spectra of ZnO powders synthesized via mechanochemical route with varying grinding times of 20, 40, and 60 minutes.

3.1.4 Field emission scanning electron microscopy

Based on the structural analysis, ZnO-NPs were found in crystalline form, but the presence of the remnants could be affecting the agglomeration of the particles. The above is exemplified in the micrographs of Figure 4a, 4b and 4c, which show the ZnO-NPs obtained after 20, 40 and 60 min of milling, respectively. ZnO-NPs of 20 min present an irregular morphology. For the samples of 40 and 60 minutes, a semi-spherical shape is observed, but decreasing in size as the milling time increases. 100 measurements were conducted for the size distribution, and according to the results they have a predominant size of 60 ±8, 40 ±3 and 30 ±2 nm for 20, 40 and 60 minutes, respectively.

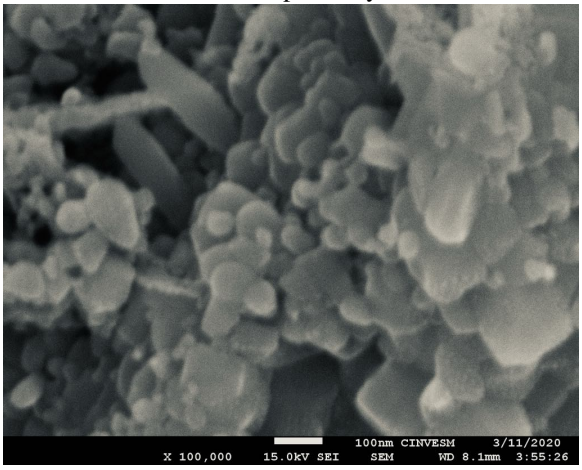

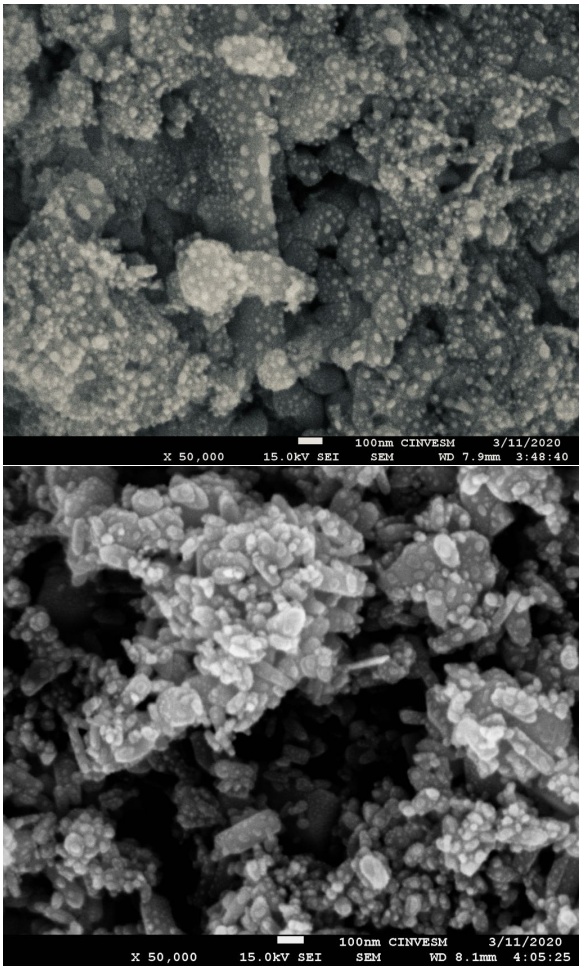

Figure 4. FESEM images of ZnO-NPs synthesized by mechanochemical route, with varying grinding times: a) 20 minutes, b) 40 minutes, and c) 60 minutes.

3.1.5 ZETA potential

Once the shape and size were identified, the size of the ZnO-NPs in suspension was confirmed. Figure 5 exhibits the distribution of particle sizes measured in solution at a concentration of 5 mg of material in 10 mL of dispersant, one for each milling time. The particle size varies for all samples, in the case for ZnO synthesized at 20 minutes the size is 373.7 nm, for ZnO synthesized at 40 minutes the size is 661.5 nm and for ZnO synthesized at 60 minutes the size is 336.2 nm. These results reveal that the nanoparticles synthesized at 60 minutes of milling have a smaller size and could have greater stability in a solution, since larger and heavier particles tend to settle more rapidly (Arenas Gaviria, 2024). The particle size of ZnO determined by this technique differs from FESEM analyses, because in the presence of water, ZnO-NPs could be disperse or aggregate depending on the pH and concentration in suspension; although ZnO does not swell, interaction with water can affect its size and shape due to the adsorption of water molecules on its surface (Salas *et al*., 2016).

Table 3. BET physicochemical characterization of ZnO-NPs, including specific surface area, pore volume, and pore size distribution in agglomerate.

Sample	Specific area (m^2/g)	Pore volume (cm^3/g)	Pore size (nm)
ZnO-20	1.75	5.15 $X10^{-3}$	25.63
ZnO-40	2.88	7.97 $X10^{-3}$	24.56
ZnO-60	7.26	21.63 $X10^{-3}$	15.53

Table 4. Average value and standard deviation of apparent viscosity (cP).

Before hot rolling																		
	25 °C						50 °C						70 °C					
	Zn-60		Zn-40		Zn-20		Zn-60		Zn-40		Zn-20		Zn-60		Zn-40		Zn-20	
C	A	SD	A	SD	A	SD	A	SD	A	SD	A	SD	A	SD	A	SD	A	SD
0	19	1	19	1	19	1	12.5	0	12.5	0	12.5	0	13.8	0.3	13.8	0.3	13.8	0.3
0.05	39	0.5	29.7	0.3	27.3	0.29	35	0.3	27	0.5	24	0	33	0.5	23.2	0.3	21.5	0.5
0.1	33.2	0.7	32	0	28.5	0	29.2	0.3	24.5	0.5	25.8	0.6	26.3	0.8	22.2	0.6	25.3	0.6
0.15	31	0.5	30	0.5	27.7	0.3	26.5	0.5	25.2	0.3	23.8	0.8	24.2	0.3	21.5	0	23.3	0.3
After hot rolling																		
0	21	0.5	21	0.5	21	0.5	18.5	1	18.5	1	18.5	1	13.5	0	13.5	0	13.5	0
0.05	37.7	0.6	36.5	0.6	33	0.3	29.2	0	27	0.6	25	0.3	25.5	0.5	24.5	0.3	23	0
0.1	39.5	0.5	36.5	0.6	36	0.5	31.5	0	31	0.8	27.5	0	28.5	0.5	23	0	25.5	0
0.15	41.2	0.8	34.5	0.3	31.5	0	31.5	0.5	25	0.6	26.5	0	26.5	0	22	0.3	22	0.3

A= Average, SD= Standard deviation, C= Concentration, ZnO-60= ZnO of 60 minutes of grinding, ZnO-40= ZnO of 40 minutes of grinding and ZnO-20= ZnO of 20 minutes of grinding.

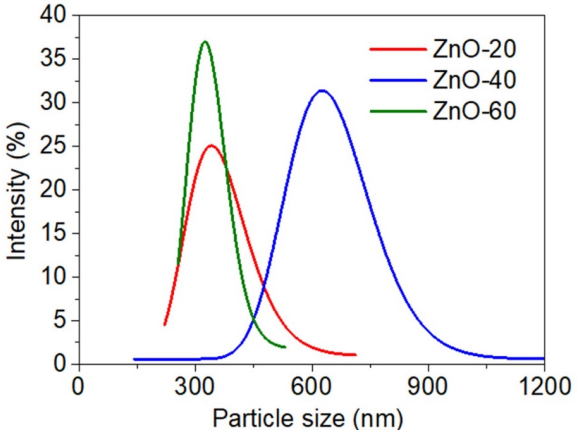

Figure 5. Particle size distribution analysis of ZnO powders synthesized via mechanochemical route, determined by Z potential measurements, using a 10 mL dispersion containing 5 mg of ZnO powder, obtained after 20, 40, and 60 minutes of grinding.

3.1.6 *Textural evaluation of the surface of ZnO-NPs by nitrogen physisorption*

All samples follow typical type IV isotherms, which are characteristic of mesoporous particles (Sing *et al.*, 1985). However, the specific area of ZnO-NPs synthesized at 60 minutes (7.26 m^2/g) is higher than that of ZnO-NPs synthesized at 20 (1.75 m^2/g) and 40 minutes (2.88 m^2/g) of milling (Table 3). This result is expected since the nanoparticles of smaller size are those synthesized at 60 minutes and it can be observed that the smaller the particle size is, the greater the specific area (Ovando, 2018).

3.2 *Evaluation of rheological and filtration properties of drilling fluid*

The results of the evaluation of Rheological properties, Filtration properties and Colloidal stability of drilling fluid for WBDF and MWBDF at 0.05, 0.10 and 0.15 % are shown below.

3.2.1 *Rheological properties*

To evaluate the effect of the ZnO-NPs addition in the WBDF, several tests were performed: apparent viscosity, plastic viscosity, yield point and gel strength at 25, 50 and 70 °C, varying the addition of the ZnO-NPs before and after rolling.

Apparent viscosity (AV) is an important parameter in hydraulic calculations, it must be adequate to lift formation cuttings and to remain between 20 and 60 cP, to ensure adequate hole cleaning capacity and well pressure control. However, these values must be adjusted depending on the specific well conditions.

Figure 6 shows the apparent viscosity (AV) for both the WBDF and the MWBDF with 0.05 %, 0.10 %, and 0.15 % w/v of ZnO-NPs, and at three different evaluated temperatures (Table 4). It is observed that at all three temperatures, the ZnO-NPs-based fluid has higher values than the WBDF. However, the MWBDF with ZnO-NPs synthesized at 60 minutes of milling and a concentration of 0.05 % demonstrates the highest AV of all temperatures. This trend persists after the fluid is submitted to hot rolling, although, in this case, the highest AV is observed at a concentration

of 0.15 %, with a tendency to degrade due to the effects of temperature.

Regarding the impact of ZnO-NPs on AV, an improvement is observed at the NPs concentration compared to the WBDF. This increase is due to the agglomeration of particles in solution (F. Duan *et al*., 2011), while at elevated temperatures it presents an inverse result since the value of AV decreases as temperature increases, this is caused by the deficiency of the intermolecular attractive forces between the nanoparticles and the WBDF (Dejtaradon *et al*., 2019).

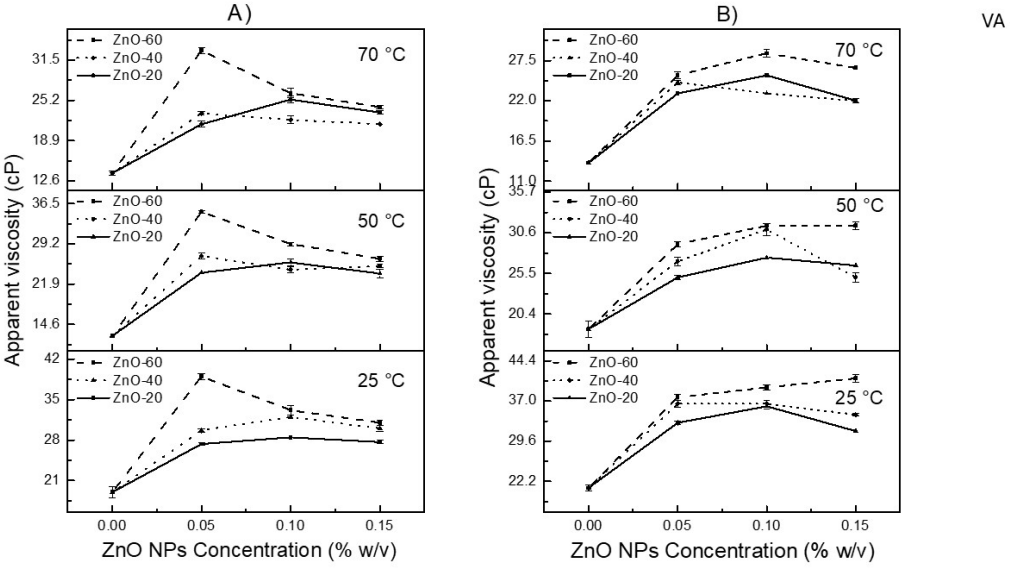

Figure 6. Rheological comparison of the base fluid (WBDF) and ZnO-NPs-based drilling fluid at varying concentrations (0.05, 0.10, and 0.15% w/v) and temperatures (70, 50, and 25 °C), before hot rolling and (A) after hot rolling (B) conditions.

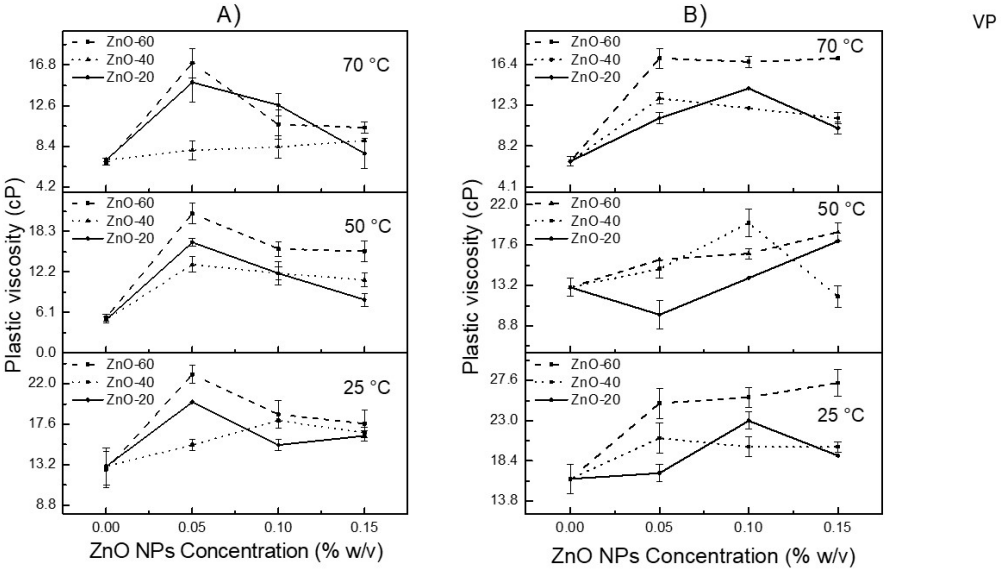

Figure 7. Comparison of the plastic viscosity enhancement of ZnO-NPs-based drilling fluids at varying concentrations (0.05, 0.10, and 0.15 % w/v) and temperatures (70, 50, and 25 °C), relative to the base fluid (BF), before hot rolling and (A) after hot rolling (B) conditions.

The AV of the MWBDF with NPs synthesized at 60 min showed an AV of 20 and 30% higher than the formulations based on NPs synthesized at 40 and 20 min respectively, for all NPs concentrations. This may be because the size of the NPs synthesized at 60 min is smaller compared to the size of those synthesized at 40 and 20 min, and the surface area being larger. This behavior aligns with that reported by Faisal *et al*., in 2024 with the work of uncoated and polymer-coated green magnetite nanoparticles and by Blkor *et al*., in 2021 in their investigation of aqueous mud with polypropylene beads and treated nanosilica treated with sodium carbonate (Blkoor *et al*., 2021; Faisal *et al*., 2024).

Plastic viscosity (PV) represents the flow resistance of drilling fluid caused by mechanical friction within the mud. According to the literature, any increase in solid content of the mud results in higher plastic viscosity (Darley & Gray, 1988). This outcome is evident in Figure 7, where nanoparticle-based fluids reach a significant increase in PV compared to the WBDF, being the highest value observed in the MWBDF with ZnO-NPs synthesized at 60 minutes. For all fluid formulations, PV decreases as the temperature increases (Table 5). At 70 °C, the MWBDF with ZnO-NPs at 40 minutes displays values similar to the WBDF, as the fluid loses thermal stability for this property. After hot rolling Figure 7b, PV values increase compared to PV before rolling. Nonetheless, the MWBDF ZnO-60-NPs fluid generally remains superior to other formulations.

The cationic ZnO-NPs interact with the anionic bentonite plates, causing the formation of larger particles within the drilling fluid. Larger particle sizes result in lower viscosity because mechanical friction is reduced (Guan *et al*., 2020). However, other studies suggest that this formation is limited by the presence of positive potassium ions, which may bind to the anionic bentonite plates (Ahasan *et al*., 2022).

The **yield point** (YP) indicates the initial resistance of the fluid caused by electrochemical forces between particles. Figure 8 shows graphs of this parameter at the three temperatures, showing that the fluid formulations based on ZnO-NPs maintain values above the WBDF (Table 6).

Table 5. Average value and standard deviation of plastic viscosity (cP).

Before hot rolling																		
	25 °C						50 °C						70 °C					
	ZnO-60		ZnO-40		ZnO-20		ZnO-60		ZnO-40		ZnO-20		ZnO-60		ZnO-40		ZnO-20	
C	A	SD	A	SD	A	SD	A	SD	A	SD	A	SD	A	SD	A	SD	A	SD
0	12.7	2	13	2	13	2	5.3	0.5	5	0.5	5	0.5	6.7	0.2	7	0.2	7	0.2
0.05	23	1	15.3	0.6	20	0	21	1.5	13.3	1.2	16.7	0.6	17	1.5	8	1	15	2
0.1	18.7	1.5	18	0	15.3	0.6	15.7	1.2	12	1	12	1.7	10.7	1.5	8.3	1.2	12.7	1.2
0.15	17.7	1.5	16.7	0.6	16.3	0.6	15.3	1.5	11	1	8	1	10.3	0.6	9	0	7.7	1.5
After hot rolling																		
0	16.3	1.7	16.3	1.7	16.3	1.7	13	1	13	1	13	1	6.7	0.5	6.7	0.5	6.7	0.5
0.05	25	1.7	21	1.7	17	1	16	0	15	1	10	1.5	17	1	13	0.6	11	0.6
0.1	25.7	1.2	20	1.2	23	1	16.7	0.6	20	1.5	14	0	16.7	0.6	12	0	14	0
0.15	27.3	1.5	20	0.6	19	0	19	1	12	1.2	18	0	17	0	11	0.6	10	0.6

A= Average, SD= Standard deviation, C= Concentration, ZnO-60= ZnO of 60 minutes of grinding, ZnO-40= ZnO of 40 minutes of grinding and ZnO-20= ZnO of 20 minutes of grinding.

Table 6. Average value and standard deviation of yield point (Pa).

Before hot rolling																		
	25 °C						50 °C						70 °C					
	ZnO-60		ZnO-40		ZnO-20		ZnO-60		ZnO-40		ZnO-20		ZnO-60		ZnO-40		ZnO-20	
C	A	SD	A	SD	A	SD	A	SD	A	SD	A	SD	A	SD	A	SD	A	SD
0	6	1.2	6	1.2	6	1.2	6.8	0.3	6.8	0.3	6.8	0.3	6.8	0.1	6.8	0.1	6.8	0.1
0.05	14.9	0.8	13.8	0.3	7	0.3	13.6	1.2	13.1	0.7	7	0.6	14.6	1	14.6	0.7	6.2	1.4
0.1	13.9	0.8	13.4	0	12.6	0.6	13	0.8	12	0.5	13.3	1.1	15	1	13.3	0.6	12.2	0.6
0.15	12.8	1	12.8	0.3	10.9	0.3	10.7	1	13.6	0.7	15.2	0.3	13.3	0.3	12	0	15	1.2
After hot rolling																		
0	5.4	2.2	5.4	2.2	5.4	2.2	5.3	0.5	5.3	0.5	5.3	0.5	6.6	0.3	6.6	0.3	6.6	0.3
0.05	12.2	1.1	13.6	1.1	15.2	1	12.6	0.3	10.9	0.6	14.9	1.3	8.2	0.5	10.9	0.3	11.8	0.6
0.1	13.3	0.7	15.5	0.6	13	0.5	14.2	0.6	11.4	0.7	13	0	11.4	0.3	10.6	0	11	0
0.15	13.3	0.7	14.2	0.3	12	0	12	0.5	12.8	0.6	8.2	0	9.1	0	10.6	0.5	11.7	0.3

A= Average, SD= Standard deviation, C= Concentration, ZnO-60= ZnO of 60 minutes of grinding, ZnO-40= ZnO of 40 minutes of grinding and ZnO-20= ZnO of 20 minutes of grinding.

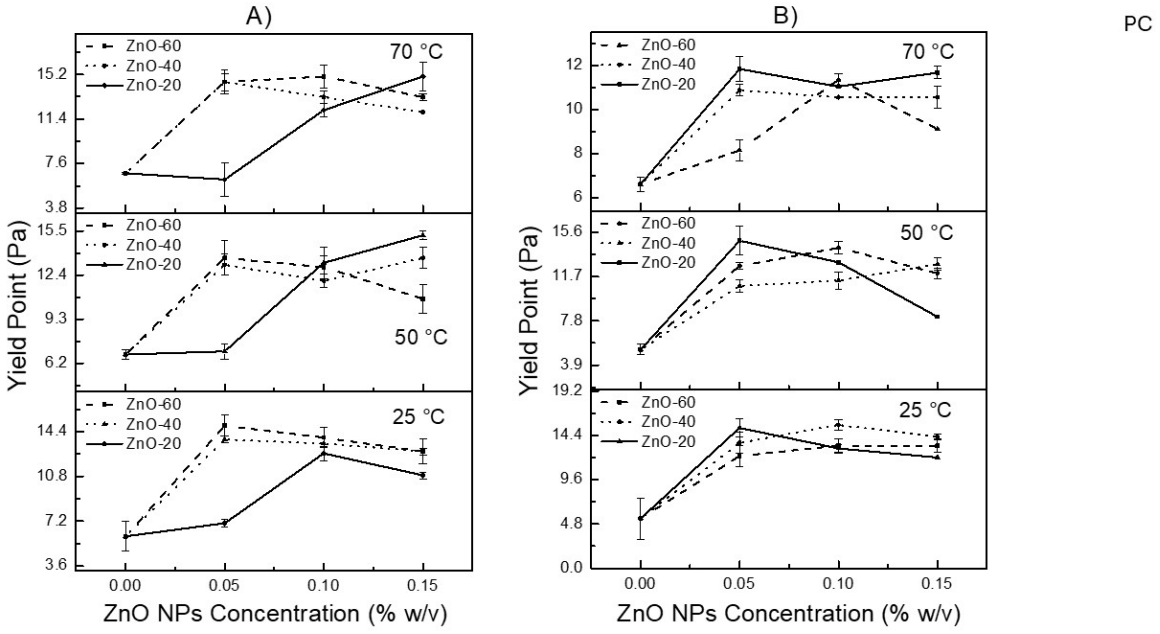

Figure 8. Comparison of the yield point of the base fluid (WBDF) and ZnO-NPs-based drilling fluid at varying concentrations (0.05, 0.10, and 0.15 % w/v) and temperatures (70, 50, and 25 °C), before hot rolling and (A) after hot rolling (B) conditions.

The graphs of the MWBDF with NPs synthesized at 40 and 60 min have similar values to those of 0.05% w/v. With this concentration, the MWBDF with NPs at 20 min and the WBDF do not exhibit a significant difference, there is only an increase in the yield point with a rise in the concentration of ZnO-NPs. After hot rolling, the MWBDF with ZnO-NPs presents an increase in the yield point compared to the WBDF, with a tendency to decrease when temperature rises.

This increase is attributed to the interaction between cationic nanoparticles on the surface and the anionic platelets of bentonite clay, triggering flocculation, which contributes to flow resistance (Baik & Lee, 2010; Barry *et al*., 2015). This means, the viscosity and the internal attraction force of the fluid increase. The surface area of materials expands at the nanoscale, and as a result, the surface energy increases. Therefore, the particles agglomerate together to reduce this energy. In other words, the attraction between the particles grows, thereby increasing the yield point by adding nanocomposites into the fluid (Hyne, 2014). The increase in yield point improves the fluid quality by enhancing the ability to clean drill cuttings from the well, reducing the probability of drillstring sticking, and reducing drillstring torque.

Gel strength is the shear stress of drilling mud that is measured at a low shear rate after the mud remains static for a certain period of time. This property allows the fluid to turn into a gel and maintain the particles and cuts generated during drilling in suspension, when there is no circulation, or the flow is interrupted (Admin, 2022).

A drilling fluid formulation designed with incorrect gel strengths often results in bit balling and settling of the drilled cutting at the bottom of the well (Ahmad *et al*., 2021). This leads to operation problems such as adhesion problems in pipes, excessive pressure and torque, and rise of bit temperature that reduces the lifespan of the tool (Admin, 2022) and causes delayed drilling operations. The main purpose of the gel strength is to suspend the drilled cutting in the wellbore during a small interruption in the drilling process; therefore, drilling formulations that keep the drilled cuttings in suspension are considered optimal (Ahmad *et al*., 2021).

Figure 9 shows the variation of gel forces for 10 minutes and 10 seconds in WBDF and MWBDF samples with the three milling times (20, 40 and 60 min) and concentration variation of the ZnO-NPs in the formulated drilling fluid (C1= C2= and C3=) and the temperature (25, 50 and 70 °C). It is observed that at the different temperatures that were evaluated, the values of this property increase for all concentrations, in contrast to the WBDF, which remains below half the value obtained with the MWBDF samples (Table 7). The fluid with the greatest gel strength is the one formulated at a concentration of 0.05 % with nanoparticles synthesized for 60 minutes of milling time. This is attributed to the fact that the surface area is greater and therefore the number of NPs per unit of weight is higher than that of the NPs synthesized at 20 and 40 minutes of milling, thus increasing the strength

of the gel in comparison with formulations with these latter NPs (Perween *et al*., 2018). After hot rolling, these values decrease due to the degradation of the additives under these temperatures and pressures. Gel strength values decrease as the temperature increases; other studies have reported similar trends (Bayat & Shams, 2019; Dejtaradon *et al*., 2019). Furthermore, progressive behavior of gel strength is observed after time, since gel strength values at 10 minutes are higher than those for the gel strength at 10 seconds; this increase is consequence of the presence of ZnO-NPs and electrostatic forces between particles in the solution (Parizad *et al*., 2018). This effect reveals the ability of the mud to suspend cuttings or drilled solids and any relatively heavy material when circulation is stopped. Although, on the other hand, greater shear force is necessary to break the gel as mud that returns to its liquid state when the drilling operation is resumed, is required.

On the other hand, comparing the rheological behavior as a function of the concentration of nanoparticles, it is observed that when it increases, the values of the rheological properties decrease. Table 8 shows evidence of this and Figure 10 presents the TEM images of ZnO-NPs obtained in the drilling fluid samples at the concentrations studied in this work, it is observed that as the concentration in the fluid sample increases, ZnO-NPs tend to agglomerate. This phenomenon is produced by the specific dynamic interactions of ZnO nanoparticles, which have surface charges that at high concentrations, can generate attraction between opposite particles, facilitating agglomeration (Aquino *et al*., 2018; Abrica and Gómez, 2022).

The enhanced rheological properties resulted from the formulations based on ZnO-NPs with a larger surface area (7.26 m^2/g), which coincides with other reports where a smaller particle size (30 nm) allows

Table 7. Average value and standard deviation of gel strength 10 seconds and 10 minutes (Pa).

		Gel strength 10 Seconds (Pa)						Gel strength 10 minutes (Pa)					
		Before hot rolling			After hot rolling			Before hot rolling			After hot rolling		
	T (°C)	25	50	70	25	50	70	25	50	70	25	50	70
WBDF	A	2.4	1.9	1.9	2.9	1.9	1.9	7	6	5.8	5.5	4.8	5.5
	SD	0.6	0	1	0.6	0.6	0.6	0.7	0.7	1.4	0.7	0	2.1
60-C1	A	6.7	6.2	5.6	6.2	5.9	4.8	10.9	10.2	9.6	9.6	9.1	8.2
	SD	0.6	0	0	0.6	1	0	1.2	1.5	0.6	0.7	0	0.7
60-C2	A	6.5	6.2	5.6	5.3	5.8	4.5	10.8	10.1	9.1	9.1	8.9	8.2
	SD	2.9	0	0.6	0.6	0	0.6	7.8	0.7	1.4	0.7	0.7	2.8
60-C3	A	6.1	5.8	5.3	5.1	4.3	4.3	10.2	9.6	8.6	9.1	8.6	7.2
	SD	0.6	0	0	0	0.6	1	1.2	1.2	0	0.7	1.4	0
40-C1	A	6.2	5.1	5.4	5.9	4.3	4.3	10.1	9.6	9.1	9.1	8.6	7.9
	SD	0	10.8	5.1	4.3	0	0	0	0	3.6	3.1	6.1	3.8
40-C2	A	5.8	5	4.5	5.3	4.3	3.8	9.4	8.9	8.6	8.6	7.7	7.7
	SD	8.3	6.2	6.2	4.7	0	0	3.6	3.8	7.9	0	0	0
40-C3	A	5.4	4.5	4.3	4.8	3.8	3.4	8.4	8.6	8.2	8.2	7	6.7
	SD	5.1	5.6	0	0	0	0	4	3.8	0	0	4.9	0
20-C1	A	6	5.1	5.3	5.4	4.3	4.3	9.6	9.1	8.9	8.9	8.6	7.2
	SD	0.7	1.4	0	1	0.6	0	0.7	1.4	0	1.4	0.7	0.7
20-C2	A	5.8	4.6	5	4.8	4.1	3.8	9.4	9.1	8.6	8.6	7.9	7.2
	SD	0.6	0.6	0	0.6	0	0.6	0	1.4	0	1.4	0.7	1.7
20-C3	A	5.4	4.5	5	4.6	3.8	3.4	9.1	8.9	8.2	8.6	7.2	6.7
	SD	0.6	0.6	0.6	0.6	0	0	0	0	0.7	0	0	1.7

A= Average, SD= Standard deviation, WBDF = water-based drilling fluid, C (1, 2 and 3) = Concentrations (0.05, 0.10, and 0.15 %) and Grinding Times (20, 40, and 60 minutes).

Table 8. Particle size of ZnO-NPs at different concentrations in drilling fluid samples, determined by Dynamic Light Scattering (DLS).

ZnO-NPs	Z-average (d.nm)	St Dev (d.nm)
60-C1	523.1	184.4
60-C2	550.1	272.4
60-C3	641.9	285.2

C1= Concentration de 0.05 %, C1= Concentration de 0.10 %, C1= Concentration de 0.15 % w/v.

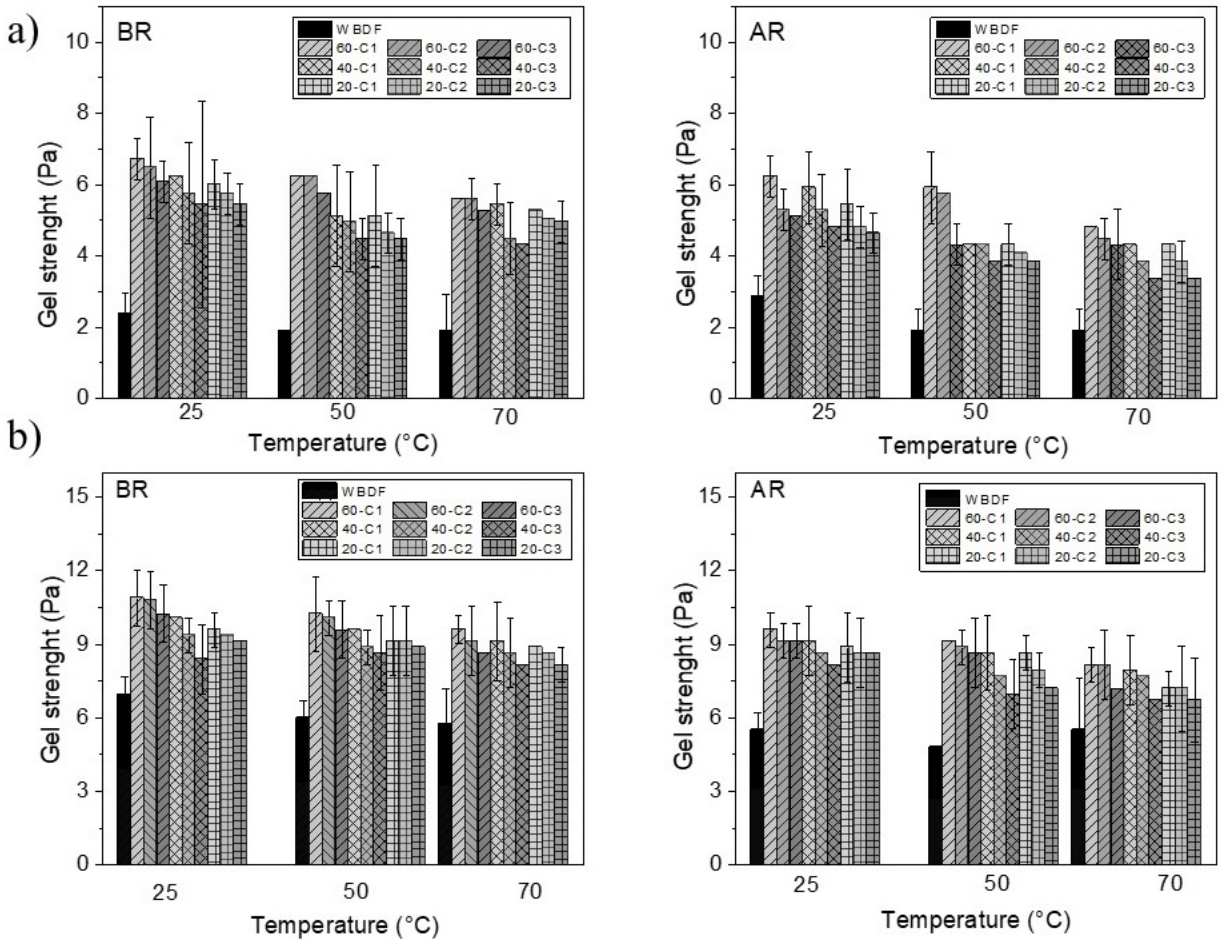

Figure 9. Gel strength behavior of ZnO-NPs-enhanced drilling fluids subjected to various temperatures. Gel strength of a) 10 seconds, b) 10 minutes of the base fluid (WBDF) and the drilling fluid based on ZnO nanoparticles at 0.05, 0.1 and 0.15 % w/v; at 25, 50 and 70 °C.

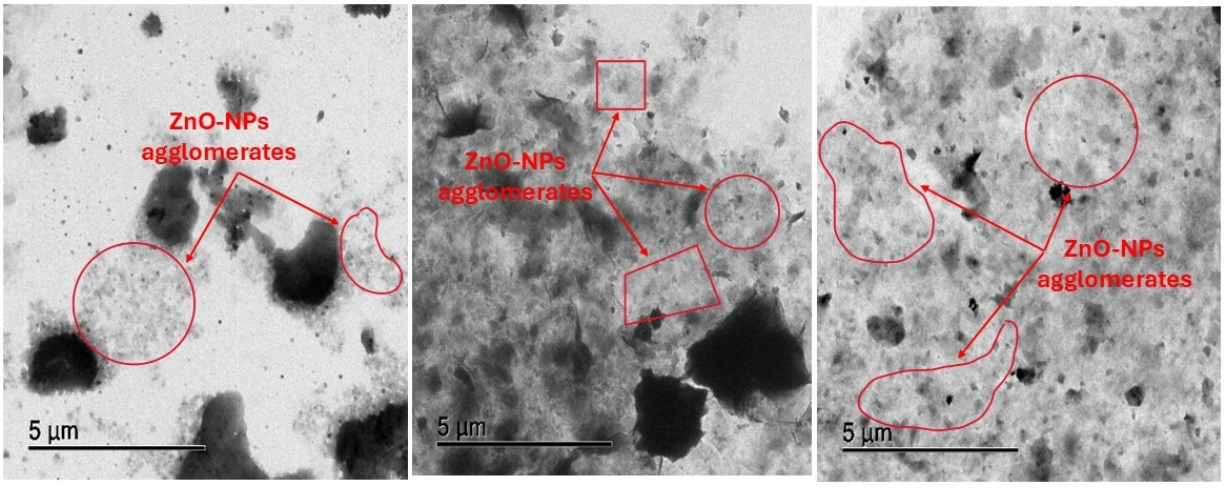

Figure 10. TEM images of ZnO-NPs synthesized by mechanochemical method at 60 minutes of grinding and suspended in drill fluid samples with concentration of (a) 0.05 %, (b) 0.10 %, (c) 0.15 % w/v.

an increase in apparent viscosity and the gel strenght of the drilling fluid (Perween *et al*., 2018), since its interruption in the clay network is less. Additionally, a drilling fluid containing particles smaller than the formation's pore diameters allows for better plugging and forms a thin, impermeable cake, reducing filtrate loss.

Another important characteristic is the specific

area of the nanoparticles that provides thermal stability to the drilling fluid due to the large number of particles per given concentration. According to Dejtaradon *et al*., (2019), the nanoparticles in the drilling fluid are required to remain stable and suspended, so it is crucial that the particle size in suspension is smaller to prevent sedimentation (Dejtaradon *et al*., (2019). These results exhibit a rheological trend similar to previous studies with oxide/polyacrylamide nanosheet nanocomposites evaluated on the properties of a WBDF and the effect of wheat nanobiopolymers on the rheological and filtration properties of the drilling fluid (Ali *et al*., 2024; Gudarzifar *et al*., 2020), Table 9 shows a comparison of rheological enhancement, filtration control, thermal stability and environmental impact of ZnO-NPs obtained in this work with other nanomaterials used in drilling fluids. In conclusion, the results obtained from this research could improve the rheological properties of WBDF more than some materials reported previously for the formulation of drilling fluids.

3.2.2 Filtration properties

Fluid loss is monitored during drilling operation as it causes problems including formation damage, stuck pipes, wellbore instability, etc. Hence, Figure 11 represents the loss of fluid at a pressure of 100 psi and 25 °C. It is observed that with the addition of ZnO-NPs the filtered volume, accumulated during the 30 minutes of the test, decreases from 13.5 to 10.4 mL. After rolling, the same trend is observed, but only with values on the lost volume from 15.2 to 12 mL (Table 10).

Table 9. Comparison of rheological enhancement, filtration control, thermal stability and environmental impact of ZnO-NPs obtained in this work with other commonly used nanomaterials in drilling fluids.

Nanomaterials	Rheological improvement	Filtration control	Thermal stability	Environmental impact
ZnO-NPs	The apparent viscosity (AV) increases by 200 %, the plastic viscosity (PV) by 180 %, and the yield point (YP) by 240% (this work).	The amount of filtered fluid lowers from 13.5 to 10.4 mL. At high pressure and high temperature, the filtered volume is reduced by 54 % (this work).	As the temperature increases, colloidal stability is maintained, although the ZnO-NPs tend to degrade, affecting the properties of the WBDF (this work).	At high concentrations, nanoparticles can pose risks to the environment (this work).
SiO_2	Apparent viscosity and yield point, in a range of 18 % to 47 %(Cardenas, 2022).	Filtration volume at 25 °C and 400 psi decreases by 19 % (Parizad *et al*., 2018)	Destabilization of colloidal dispersion occurs due to increased temperature (Parizad *et al*., 2018).	SiO_2 is considered environmentally safe, especially if used in biodegradable combinations (Cardenas, 2022).
TiO_2	TiO_2-NPs contributes to an increase in the viscosity(Sadeghalvaad & Sabbaghi, 2015).	The volume of filtrate loss decreased by 64 % with the addition of NPs. (Sadeghalvaad & Sabbaghi, 2015).	They have resistance to thermal degradation in the rheological and filtration characteristics of drilling fluids (Beg *et al*., 2020).	TiO_2 nanoparticles can increase the thermal stability of drilling fluid, at high temperature they have little degradation (Mendoza & Rojas, 2021).
Graphene oxide (GO)	The plastic viscosity of the drilling fluid increased reaching 15 and 18 mPa·s, The YP of the drilling fluids increased with NPs (Abdullah *et al*., 2024).	Filtration loss decreased to 38.96 % and 34.36 %, at LPLT and HPHT, respectively (Gudarzifar *et al*., 2020).	The side chains, like the main chains of the nanocomposite, remain stable at high temperaturas (Abdullah *et al*., 2024).	It is thermally more stable with synthesized additives (Gudarzifar *et al*., 2020).
Carbon nanotubes	Plastic viscosity improved by 85.7 % and gel characteristics by more than 160 % (Lysakova *et al*., 2025).	HTHP filtration loss was reduced by 42.86 % 11 % reduction in API filtration loss (Lysakova *et al*., 2025).	The properties of the fluids deteriorated with increasing temperatura (Lysakova *et al*., 2025).	They are more environmentally friendly than their petroleum-based counterparts (Lysakova *et al*., 2025).

Table 10. Average value and standard deviation of volume of filtrate in mL, under Low-Pressure (100 psi) and Low-Temperature (25 °C) Conditions.

Before hot rolling																				
	BF		60-C1		60-C2		60-C3		40-C1		40-C2		40-C3		20-C1		20-C2		20-C3	
Time min	A	SD	A	SD	A	SD	A	SD	A	SD	A	SD	A	SD	A	SD	A	SD	A	SD
0	0	0	0	0	0	0	0	0	0	0	0	0	0	0	0	0	0	0	0	0
5	5	0.2	3.6	0.2	4.8	0.3	4.2	0.6	4.2	0.2	4.4	0.3	4.6	0.4	4.2	0.6	4.6	0.5	4.4	0.6
10	6.8	0.4	5.4	0.4	6.4	0.5	6.6	0.7	6	0.7	6.4	0.6	6.6	0.6	6.4	0.5	6	0.1	6.2	0.2
15	8.5	0.5	7	0.2	7.8	0.4	8	0.3	7.6	0.4	8	0.3	8.2	0.4	7.6	0.3	7.8	0.3	8	0.4
20	10.2	0.3	8.3	0.1	9.2	0.3	9.4	0.4	9	0.3	9.4	0.3	9.4	0.4	8.8	0.4	9	0.1	9.2	0.4
25	11.9	0.4	9.4	0.1	10	0.3	10.6	0.5	10.2	0.3	10.5	0.6	10.2	0.2	10.6	0.5	10	0.4	10.6	0.5
30	13.5	0.5	10.4	0.3	11.2	0.5	11.6	0.2	11.2	0.4	11.6	0.8	11.6	0.5	11.8	0.4	11.2	0.4	11.4	0.2
Before hot rolling																				
0	0	0	0	0	0	0	0	0	0	0	0	0	0	0	0	0	0	0	0	0
5	6	0.4	5	0.2	4.6	0.7	6	0.2	5.6	0.6	4.8	0.4	4.6	0.5	5.4	0.2	5.7	0.2	5.5	1.1
10	8.3	0.5	7	0.7	8.2	0.4	8.6	0.7	7.8	0.3	8.2	0.5	8	0.2	8	0.1	7.6	0.8	7.8	0.6
15	10.8	0.7	8.8	0.7	9.8	0.7	10.6	0.7	9.6	0.6	10	0.5	9.8	0.8	9.8	0.2	10	1.5	9.5	0.5
20	12.5	0.6	9.6	0.2	11.6	0.6	12.2	0.5	10.8	0.6	11.6	0.8	11.6	0.3	11.2	0.5	11.8	1	11	0.6
25	13.6	0.6	10.8	0.4	12.8	0.8	13.4	0.5	12	0.2	12.8	0.2	12.8	0.8	12.6	0.8	12.8	0.2	12.5	0.9
30	15.2	1.2	12	0.4	13.2	0.3	14.8	0.9	13.2	0.4	14.2	0.5	14.5	0.5	13.8	1	14.1	0.5	13.8	0.8

A= Average, SD= Standard deviation, WBDF = Base fluid, C (1, 2 y 3) = Concentrations (0.05, 0.1, and 0.15%) and Grinding Times (20, 40, and 60 minutes).

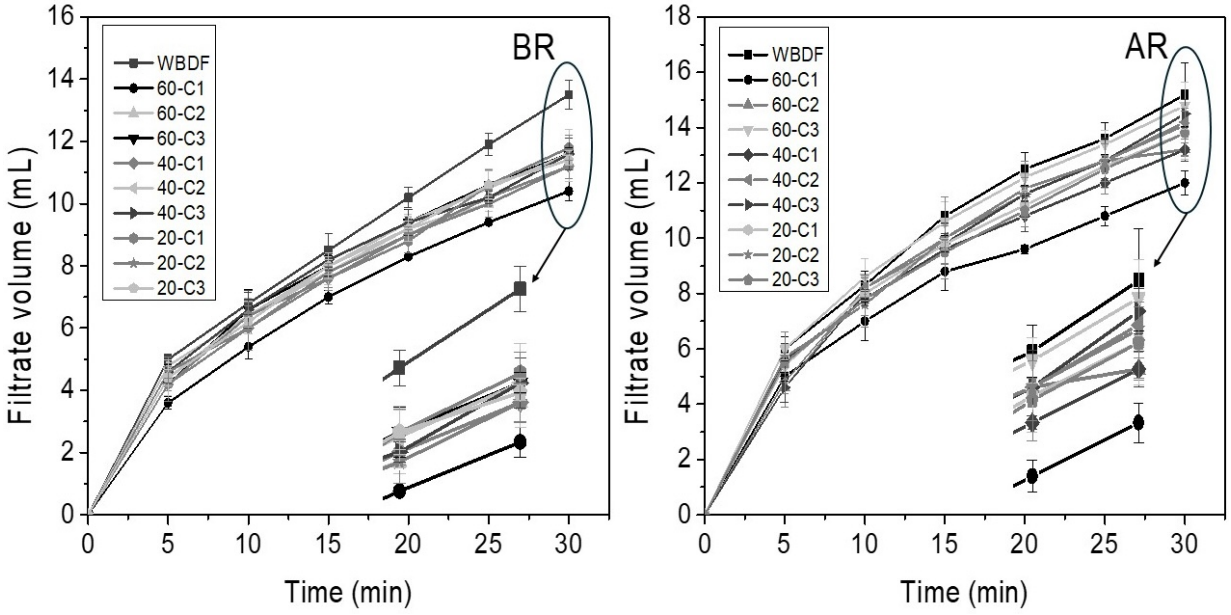

Figure 11. Filtration performance of WBDF and ZnO-NPs-enhanced drilling fluids at various concentrations (0.05, 0.10, and 0.15 % w/v) and grinding times (20, 40, and 60 minutes), Under Low-Pressure (100 psi) and Low-Temperature (25 °C) Conditions.

The formulation of the drilling fluid with the largest volume of filtrate reduction is the fluid with ZnO-NPs of 60 minutes of milling and concentration of 0.05 (60-C1). This is because with this concentration the filter cake that is formed is a thin and impermeable suitable filter cake, in other words, the nanoparticles are filling the pores of the formation, preventing the passage of fluid into the formation (Ahmed *et al*., 2020).

Each cake obtained was measured using an accuracy vernier caliper and Table 11 lists the thicknesses in inches (in) of the cake obtained after the low pressure and temperature filtration test. It can be seen that the thickness is reduced to around 50 % with the addition of the ZnO-NPs compared to the WBDF. Moreover, there is a change in appearance and color as seen in the images in Figure 12.

Regarding the lost filtration test, Figure 13 illustrates the volume filtered at high pressure and high temperature, before and after rolling, for all samples of the WBDF and the drilling fluid with the addition of 0.05, 0.10 and 0.15 % w/v of ZnO-NPs with

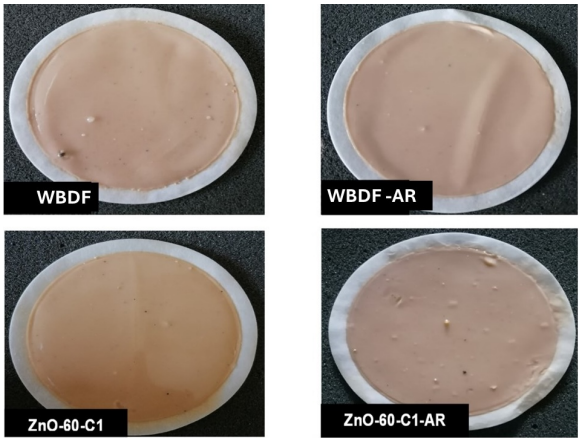

Figure 12. Photograph of filter cakes of the WBDF and with ZnO-NPs, before and after hot rolling.

Table 11. Evaluation of filter cake thickness in ZnO-enhanced drilling fluid formulations: before and after rolling process.

Formulations	Before rolling (mm)	After rolling (mm)
ZnO-20-C1	1.295	1.397
ZnO-20-C2	1.346	1.651
ZnO-20-C3	1.854	2.159
ZnO-40-C1	1.27	1.778
ZnO-40-C2	1.27	1.651
ZnO-40-C3	1.575	2.388
ZnO-60-C1	1.194	1.27
ZnO-60-C2	1.346	1.956
ZnO-60-C3	1.854	2.083

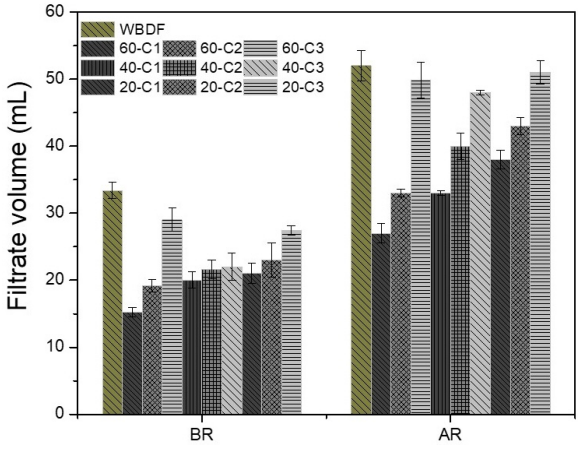

Figure 13. HPHT filtered volume analysis of WBDF and ZnO-NPs-enhanced drilling fluids at various concentrations (0.05, 0.1, and 0.15%) and grinding durations (20, 40, and 60 minutes).

milling times of 20, 40 and 60 min. The filtrate volume lost in the test carried out at 500 psi pressure and 150 °C, a significant reduction in lost volume is observed for the formulations with ZnO-NPs (Table 12). The formulation with ZnO-NPs of 60 minutes of milling was the one that showed the greatest reduction from 54 and 48 % before and after rolling. Therefore, it is assumed that the ZnO-NPs are blocking the pore spaces of the base fluid.

Filtration tests show that ZnO-NPs reduce the volume filtered into the formation; at 100 psi and room temperature, the filtered volume accumulated during the 30 minutes of the test is reduced from 13.5 to 10.4 mL (Tala 12). After hot rolling, the same trend is noticed, with a reduction from 15.2 to 12 mL. For the case of elevated pressure and temperature conditions (500 psi and 100 °C), it is reduced by 54 % (15.2 mL) and 48 % (27 mL), compared to the WBDF (33.4 and 52 mL), before and after rolling, respectively (Table 13). At a temperature of 70 °C and after hot rolling, the rheological properties of the drilling fluid decrease, however, this drop is minor compared to the WBDF.

3.2.3 Colloidal stability of drilling fluid

The colloidal stability study was carried out by visual observation (Li *et al*., 2020; Macías C. *et al*., 2024) , consisting of introducing the samples of the drilling fluid formulations into 15 mL test tubes. They were observed from the beginning and every 24 hours, for 10 days, to show the stability of the samples over time. In Figure 14, it can be seen that samples with different concentrations of ZnO-NPs synthesized at different grinding times showed better stability compared to WBDF. The nine samples of the MWBDF remained stable after 10 days, no sedimentation is observed in the test tubes, however, in the base fluid a separation of the water is observed (Figure 14d). The other formulations based on ZnO-NPs are observed without significant changes in the test tube, evidencing that the addition of these nanoparticles improves colloidal stability.

Conclusion

This study aimed to develop a water-based drilling fluid, MWBDF using ZnO-NPs as additives for this type of drilling fluids. Based on the results, it can be concluded that ZnO-NPs, synthesized by the mechanochemical method, were capable of improving the rheological and filtration properties of water-based drilling fluids. Causing this material to be versatile due to the simplicity of its synthesis and useful due to the characteristics of improvements in rheological properties. Particularly, the MWBDF with ZnO-NPs that had the best performance was the one obtained using the ZnO-NPs for 60 minutes of milling and a concentration of 0.05 in the BF, at room temperature. The other evaluated properties, in comparison to the WBDF, also reported improvements such as an increase in AV to 200 %, PV to 180 %, yield point to

240 % and gel strength increases 80 % more than the WBDF after 10 minutes of being in static condition. It was observed that concentrations of 0.10 and 0.15 % are not recommended since these nanoparticles tend to agglomerate and this deteriorates the properties. In conclusion, this improvement process is viable with only 0.05 % of ZnO-NPs in the BF.

Table 12. Average value and standard deviation of volume of filtrate HPHT.

	WBDF		60-C1		60-C2		60-C3		40-C1		40-C2		40-C3		20-C1		20-C2		20-C3	
	A	SD	A	SD	A	SD	A	SD	A	SD	A	SD	A	SD	A	SD	A	SD	A	SD
BR	33.4	1.2	15.2	0.7	19.2	0.9	29	1.7	20	1.2	21.6	1.4	22	2	21	1.5	23	2.6	27.4	0.7
AR	52	2.3	27	1.4	33	0.5	49.8	2.6	33	0.4	40	2	48	0.3	38	1.4	43	1.2	51	1.7

A= Average, SD= Standar desviation, BR= Before hot rolling, AR= After hot rolling, WBDF = Base fluid, C (1, 2 and 3) = Concentrations (0.05, 0.1, and 0.15%) and Grinding Times (20, 40, and 60 minutes).

Table 13. Comparison of filtered volume reduction in different formulations before and after hot rolling process.

Formulations	Before rolling (%)	After rolling (%)
60-C1	54	48
60-C2	43	37
60-C3	13	4
40-C1	40	37
40-C2	35	23
40-C3	34	8
20-C1	37	27
20-C2	31	17
20-C3	18	2

Figure 14. Samples of ZnO-NPs-based drilling fluid formulations and WBDF: a) day 1, b) day 5, c) day 10 and d) separation of water in the WBDF.

The fluid that gave the best result regarding the filtration property was the WBDF added with 0.05 % of ZnO-NPs synthesized at 60 minutes of milling (60-C1). It was also the one that obtained the best formed filter cake, that is, being permeable and thin, with a lower thickness of the cake formed on the filter paper after the filtration test.

As can be seen, the use of ZnO-NPs can provide significant benefits to the properties of water-based drilling fluids. However, there are also important limitations that must be considered. Obtain ZnO-NPs with controlled properties (such as specific size and morphology) through mechanochemical synthesis could be difficult to scale. Since drilling operations require a large volume of NPs, it is necessary to investigate economical and environmentally friendly synthesis methods to reduce costs. Another limitation is the compatibility of ZnO-NPs with the different conditions and properties of each reservoir and oil well. These NPs are sensitive to factors such as pH, temperature, and the presence of contaminants. In this research, field trials were not possible; it would be important to validate the laboratory results obtained and evaluate their behavior under real-world conditions. Furthermore, it was observed that at high concentrations, nanoparticles tend to agglomerate, reducing the available active surface area and decreasing their effectiveness in functions such as cuttings transport. Therefore, it is important to explore combinations of ZnO with other materials, such as TiO_2 or SiO_2, to create hybrid nanoparticles that further improve the performance of drilling fluid properties. It is also important to investigate methods to coat or functionalize nanoparticles with polymers, organic compounds, or ligands that can improve their stability and compatibility. Another issue is that nanoparticles face specific regulations related to their safe use and handling. Although ZnO is recognized for its antimicrobial capacity, at high concentrations, nanoparticles can pose risks to human health and the environment, especially if released during drilling. Therefore, it is necessary to analyze their biodegradability or ways to recover the nanoparticles after use. The use of ZnO-NPs in drilling fluids remains a promising field, although the implementation of nanoparticles in drilling fluids at the field scale faces several technical, economic and environmental challenges, and research is required to mitigate these limitations.

Acknowledgements

This research was financially supported by the Secretaría de Ciencia, Humanidades, Tecnología e Innovación (SECIHTI) in Universidad Juárez Autónoma de Tabasco.

References

Abdullah, A. H., Ridha, S., Mohshim, D. F., and Maoinser, M. A. (2024). An experimental investigation into the rheological behavior and filtration loss properties of water-based drilling fluid enhanced with a polyethyleneimine-grafted graphene oxide nanocomposite. *RSC Advances* 14(15), 10431–10444. https://doi.org/10.1039/D3RA07874D.

Abrica G., P., and Gómez A., S. (2022). Effects and characterization of airborne nanoparticles (CuO, ZnO-NPs) in plants. *Revista Internacional de Contaminacion Ambiental* 38, 145–164. https://doi.org/10.20937/RICA.54303.

Admin. *Resistencia de gel*. (2022) Available at: Https://Blog.Industriasmorven.Com/Resistencia-de-Gel/. Accessed: November 15, 2023.

Aghdam, S. B., Moslemizadeh, A., Kowsari, E., and Asghari, N. (2020). Synthesis and performance evaluation of a novel polymeric fluid loss controller in water-based drilling fluids: High-temperature and high-salinity conditions. *Journal of Natural Gas Science and Engineering 83*, 103576. https://doi.org/10.1016/j.jngse.2020.103576 .

Ahasan, M. H., Alahi Alvi, M. F., Ahmed, N. and Alam, M. S. (2022). An investigation of the effects of synthesized zinc oxide nanoparticles on the properties of water-based drilling fluid. *Petroleum Research 7*(1), 131–137. https://doi.org/10.1016/j.ptlrs.2021.08.003.

Ahmad, H. M., Iqbal, T., A. Al Harthi, M. and Kamal, M. S. (2021). Synergistic effect of polymer and nanoparticles on shale hydration and swelling performance of drilling fluids. *Journal of Petroleum Science and Engineering 205*. https://doi.org/10.1016/j.petrol.2021.108763.

Ahmed, N., Alam, M. S. and Salam, M. A. (2020). Experimental analysis of drilling fluid prepared by mixing iron (III) oxide nanoparticles with a KCl–Glycol–PHPA polymer-based mud used in drilling operation. *Journal of Petroleum Exploration and Production Technology 10*(8), 3389–3397. https://doi.org/10.1007/s13202-020-00933-1.

Ali, J. A., Abbas, D. Y., Abdalqadir, M., Nevecna, T., Jaf, P. T., Abdullah, A. D. and Rancová, A. (2024). Evaluation the effect of wheat nano-biopolymers on the rheological and

filtration properties of the drilling fluid: Towards sustainable drilling process. *Colloids and Surfaces A: Physicochemical and Engineering Aspects 683*. https://doi.org/10.1016/j.colsurfa.2023.133001.

Al-Zubaidi, N. S., Alwasiti, A. A. and Mahmood, D. (2017). A comparison of nano bentonite and some nano chemical additives to improve drilling fluid using local clay and commercial bentonites. *Egyptian Journal of Petroleum 26*(3), 811–818. https://doi.org/10.1016/j.ejpe.2016.10.015 .

API. (2019). API RP 13B-1 *manual de práctica recomendada para pruebas de campo de fluidos de perforación a base de agua.* 5th edition.

Aquino, P., Osorio, A. M., Ninán, E., and Torres, F. (2018). Characterization of ZnO nanoparticles synthesized by precipitation method and its evaluation in the incorporation in enamel paints. *Rev Soc Quím Perú* 84(1).

Arenas Gaviria, J. A. (2024). *Análisis de las propiedades fisicoquímicas y reológicas que afectan la sedimentación de suspensiones minerales en espesadores en la industria del cemento*. Universidad Nacional de Colombia.

Baik, M. H. and Lee, S. Y. (2010). Colloidal stability of bentonite clay considering surface charge properties as a function of pH and ionic strength. *Journal of Industrial and Engineering Chemistry 16*(5), 837–841. https://doi.org/10.1016/j.jiec.2010.05.002.

Barry, M. M., Jung, Y., Lee, J. K., Phuoc, T. X. and Chyu, M. K. (2015). Fluid filtration and rheological properties of nanoparticle additive and intercalated clay hybrid bentonite drilling fluids. *Journal of Petroleum Science and Engineering 127*, 338–346. https://doi.org/10.1016/j.petrol.2015.01.012.

Bayat, A. E. and Shams, R. (2019). Appraising the impacts of SiO2, ZnO and TiO2 nanoparticles on rheological properties and shale inhibition of water-based drilling muds. *Colloids and Surfaces A: Physicochemical and Engineering Aspects 581*. https://doi.org/10.1016/j.colsurfa.2019.123792.

Beg, M., Kumar, P., Choudhary, P., and Sharma, S. (2020). Effect of high temperature ageing on TiO2 nanoparticles enhanced drilling fluids: A rheological and filtration study. *Upstream Oil and Gas Technology* 5, 100019. https://doi.org/10.1016/j.upstre.2020.100019.

Blkoor, S. O., Ismail, I., Oseh, J. O., Selleyitoreea, S., Norddin, M. N. A. M., Agi, A. and Gbadamosi, A. O. (2021). Influence of polypropylene beads and sodium carbonate treated nanosilica in water-based muds for cuttings transport. *Journal of Petroleum Science and Engineering 200*. https://doi.org/10.1016/j.petrol.2021.108435.

Bolarinwa, H. S., Onuu, M. U., Fasasi, A. Y., Alayande, S. O., Animasahun, L. O., Abdulsalami, I. O., Fadodun, O. G. and Egunjobi, I. A. (2017). Determination of optical parameters of zinc oxide nanofibre deposited by electrospinning technique. *Journal of Taibah University for Science 11*(6), 1245–1258. https://doi.org/10.1016/j.jtusci.2017.01.004.

Cardenas A., W. (2022). Effect of the addition of ZnO and SiO_2 nanoparticles on the rheological properties of a water-based drilling fluid. Degree thesis to obtain the title of Chemist. Universidad industrial de Santander. https://noesis.uis.edu.co/items/0f8b9e94-98b0-442a-9aff-ea275eefdf56 .

Chuck H., C., Pérez C., E., Heredia O., E., and Serna S., S. O. (2011). Sorghum as a multifaceted crop for bioethanol production in Mexico: technologies, advances, and areas of opportunity. *Revista Mexicana de Ingeniería Química* 10 (3).

Darley, H. C. and Gray, G. R. (1988). *Composition and Properties of Drilling and Completion Fluids* (Fifth Edition). Gulf Professional Publishing.

Dejtaradon, P., Hamidi, H., Chuks, M. H., Wilkinson, D. and Rafati, R. (2019). Impact of ZnO and CuO nanoparticles on the rheological and filtration properties of water-based drilling fluid. *Colloids and Surfaces A: Physicochemical and Engineering Aspects 570*, 354–367. https://doi.org/10.1016/j.colsurfa.2019.03.050.

Duan, F., Kwek, D. and Crivoi, A. (2011). Viscosity affected by nanoparticle aggregation in Al2O3-water nanofluids. *Nanoscale Research Letters 6*(1). https://doi.org/10.1186/1556-276X-6-248.

Duan, Y., Dong, X., Yang, H., Fan, Y., Ma, X. and Lin, W. (2024). Study of solid-liquid two-phase flow model of drilling fluids for analyzing mud cake formation. *Geoenergy Science and Engineering 236*, 212761. https://doi.org/10.1016/j.geoen.2024.212761 .

Espitia, P. J. P., Soares, N. de F. F., Coimbra, J. S. dos R., de Andrade, N. J., Cruz, R. S., & Medeiros, E. A. A. (2012). Zinc Oxide Nanoparticles: Synthesis, Antimicrobial Activity and Food Packaging Applications. In Food and Bioprocess Technology (Vol. 5, Issue 5, pp. 1447–1464). https://doi.org/10.1007/s11947-012-0797-6.

Faisal, R., Kamal, I., Salih, N. and Préat, A. (2024). Optimum formulation design and properties of drilling fluids incorporated with green uncoated and polymer-coated magnetite nanoparticles. *Arabian Journal of Chemistry 17*(2). https://doi.org/10.1016/j.arabjc.2023.105492.

Friedheim, J., Young, S., De Stefano, G., Lee, J., Guo, Q. and Swaco, M.-I. (2012). Nanotechnology for Oilfield Applications-Hype or Reality?. *Society of Petroleum Engineers 157032.*

García M., R., Suárez V., G. G., Pech R., W. J., Ordóñez, L. C., Melendez G., P. C., Sánchez P., N. M., and González Q., D. (2024). Soft chemistry synthesis of size-controlled ZnO nanostructures as photoanode for dye-sensitized solar cell. *Revista Mexicana de Ingeniera Química* 23(2). https://doi.org/10.24275/rmiq/IE24235

Ghayedi, A. and Khosravi, A. (2020). Laboratory investigation of the effect of GO-ZnO nanocomposite on drilling fluid properties and its potential on H2S removal in oil reservoirs. *Journal of Petroleum Science and Engineering 184*. https://doi.org/10.1016/j.petrol.2019.106684.

Guan, O. S., Gholami, R., Raza, A., Rabiei, M., Fakhari, N., Rasouli, V. and Nabinezhad, O. (2020). A nano-particle based approach to improve filtration control of water based muds under high pressure high temperature conditions. *Petroleum 6*(1), 43–52. https://doi.org/10.1016/j.petlm.2018.10.006.

Gudarzifar, H., Sabbaghi, S., Rezvani, A. and Saboori R. (2020). Experimental investigation of rheological & filtration properties and thermal conductivity of water-based drilling fluid enhanced. *Powder Technology 368*, 323–341. https://doi.org/10.1016/j.powtec.2020.04.049.

Hyne, N. J. (2014). *Diccionario de exploración, perforación y producción de petróleo* (2nd ed.). PennWell.

Li, S., Ng, Y. H., Lau, H. C., Torsæter, O., and Stubbs, L. P. (2020). Experimental investigation of stability of silica nanoparticles at reservoir conditions for enhanced oil-recovery applications. *Nanomaterials* 10(8), 1–15. https://doi.org/10.3390/nano10081522.

Lysakova, E. I., Skorobogatova, A. D., Neverov, A. L., Pryazhnikov, M. I., Rudyak, V. Ya. and Minakov, A. V. (2024). Physico-chemical studies and development of water-based drilling fluid formulations with carbon nanotube additives. *Journal of Molecular Liquids*, 125448. https://doi.org/10.1016/j.molliq.2024.125448.

Lysakova, E. I., Skorobogatova, A. D., Neverov, A. L., and Minakov, A. V. (2025). Investigation of the effect of spherical nanoparticle additives on the properties of drilling fluids modified by carbon nanotubes. *Nano-Structures & Nano-Objects* 41, 101442. https://doi.org/10.1016/j.nanoso.2025.101442.

Ma, L., Yin, D., Ren, J., Han, B. and Qin, S. (2024). A novel thixotropic structural dynamics model of water-based drilling fluids. *Geoenergy Science and Engineering 234*, 212585. https://doi.org/10.1016/j.geoen.2023.212585.

Macías C., K., Ballesteros R., L. T., Velázquez V., V. W., Frías M., D. M., López G., R., and Alvarez L., M. A. (2024). Effect of chitosan on the electrokinetic, spectroscopic, and textural properties of TiO2 nanoparticles. *Revista Mexicana de Ingeniera Química* 23(1). https://doi.org/10.24275/rmiq/Poly24218

Martin, C., Nourian, A., Babaie, M. and Nasr, G. G. (2024). Innovative drilling fluid containing sand grafted with a cationic surfactant capable of drilling high pressure and high temperature geothermal and petroleum wells. *Geoenergy Science and Engineering 237*. https://doi.org/10.1016/j.geoen.2024.212767.

Mendoza R., M. A., and Rojas P., K. K. (2021). Nanotechnology applied in water-based drilling fluids to inhibit formation damage. Degree project for the title of petroleum engineer. Fundación Universidad de América. Chrome https://repository.uamerica.edu.co/server/api/core/bitstreams/002f5fc5-12e0-496f-8744-1a15a817d893/content .

Nwaezeapu, V. C., Ezenwaka, K. C. and Ede, T. A. (2019). Evaluation of hydrocarbon reserves using integrated petrophysical analysis and seismic interpretation: A case study of

TIM field at southwestern offshore Niger Delta oil Province, Nigeria. *Egyptian Journal of Petroleum 28*(3), 273–280. https://doi.org/10.1016/j.ejpe.2019.06.002.

Ofei, T. N., Lund, B. and Saasen, A. (2021). Effect of particle number density on rheological properties and barite sag in oil-based drilling fluids. *Journal of Petroleum Science and Engineering 206*, 108908. https://doi.org/10.1016/j.petrol.2021.108908 .

Ovando M., V. M. (2018). Facile synthesis of low band gap ZnO microstructures. *Revista Mexicana de Ingeniería Química* 17(2), 455–462. https://doi.org/10.24275/10.24275/uam/izt/dcbi/revmexingquim/2018v17n2/Ovando.

Parizad, A., Shahbazi, K. and Tanha, A. A. (2018). SiO_2 nanoparticle and KCl salt effects on filtration and thixotropical behavior of polymeric water based drilling fluid: With zeta potential and size analysis. *Results in Physics 9*, 1656–1665. https://doi.org/10.1016/j.rinp.2018.04.037 .

Perween, S., Beg, M., Shankar, R., Sharma, S. and Ranjan, A. (2018). Effect of zinc titanate nanoparticles on rheological and filtration properties of water based drilling fluids. *Journal of Petroleum Science and Engineering 170*, 844–857. https://doi.org/10.1016/j.petrol.2018.07.006.

Prieto G., F., Sánchez J., F., Méndez M., M. A., García B., G., and Gordillo M., A. J. (2007). Obtención y caracterización de ferritas ternarias de manganeso por mecanosíntesis. Boletín de La Sociedad Geológica Mexicana 59(1), 125–132. https://doi.org/10.18268/BSGM2007v59n1a10

Qi, Q., Zhang, T., Yu, Q., Wang, R., Zeng, Y., Liu, L. and Yang, H. (2008). Properties of humidity sensing ZnO nanorods-base sensor fabricated by screen-printing. *Sensors and Actuators, B: Chemical 133*(2), 638–643. https://doi.org/10.1016/j.snb.2008.03.035.

Rafati, R., Smith, S. R., Sharifi Haddad, A., Novara, R. and Hamidi, H. (2018). Effect of nanoparticles on the modifications of drilling fluids properties: A review of recent advances. In *Journal of Petroleum Science and Engineering* 161, 61–76. https://doi.org/10.1016/j.petrol.2017.11.067.

Ramos, J., Santamaría Osorio, L., Andrés Mendoza Leiva, C., Uribe, W. and Polanco, L. (2013). Almidón modificado de yuca como aditivo en fluidos de perforación base agua. *Revista Investigacion.indb* 6(1).

Reilly, S. I., Vryzas, Z., Kelessidis, V. C. and Gerogiorgis, D. I. (2016). First-principles Rheological Modelling and Parameter Estimation for Nanoparticle-based Smart Drilling Fluids. In *Computer Aided Chemical Engineering* 38, 1039–1044. https://doi.org/10.1016/B978-0-444-63428-3.50178-8.

Sadeghalvaad, M. and Sabbaghi, S. (2015). The effect of the TiO2/polyacrylamide nanocomposite on water-based drilling fluid properties. *Powder Technology 272*, 113–119. https://doi.org/10.1016/j.powtec.2014.11.032.

Salas, G., Rosas, N., Galeas, S., Guerrero, V., and Debut, A. (2016). Síntesis de Nanopartículas de ZnO por el Método de Pechini. *Revista Politécnica* 38 (1). https://www.redalyc.org/articulo.oa?id=688773643005.

Sapkota, R., Duan, P., Kumar, T., Venkataraman, A., and Papadopoulos, C. (2021). Thin film gas sensors based on planetary ball-milled zinc oxide nanoinks: Effect of milling parameters on sensing performance. *Applied Sciences (Switzerland)* 11(20). https://doi.org/10.3390/app11209676.

Senthilkumaar, S., Rajendran, K., Banerjee, S., Chini, T. K. and Sengodan, V. (2008). Influence of Mn doping on the microstructure and optical property of ZnO. *Materials Science in Semiconductor Processing 11*(1), 6–12. https://doi.org/10.1016/j.mssp.2008.04.005.

Sing, K. S. W., Everett, D. H., Haul, R. A. W., Moscou, L., Pierotti, R. A., Rouquerol, J. and Siemieniewska, T. (1985). *Reporting physisorption data for gas/solid systems-with special reference to the determination of surface area and porosity*. https://doi.org/10.1351/pac198557040603.

Sulaimon, A. A., Adeyemi, B. J., and Rahimi, M. (2017). Performance enhancement of selected vegetable oil as base fluid for drilling HPHT formation. *Journal of Petroleum Science and Engineering* 152, 49–59. https://doi.org/10.1016/j.petrol.2017.02.006.

Tichaona Taziwa, R., Leroy Meyer, E., Taziwa Taziwa, R. and Ntozakhe, L. (2017). Structural, Morphological and Raman Scattering Studies

of Carbon Doped ZnO Nanoparticles Fabricated by PSP Technique. *Journal of Nanoscience and Nanotechnology 1*(1). https://www.researchgate.net/publication/321061464.

Yi, S., Xu, Y., Cao, Y., Mao, H., He, G., Shi, H., Li, X. and Dong, H. (2024). The decisive role of filtration reducers' surface charge in affecting drilling fluid filtration performance. *Journal of Molecular Liquids 409*, 125505. https://doi.org/10.1016/j.molliq.2024.125505.

Zargar, R. A., Khan, S. U. D., Khan, M. S., Arora, M. and Hafiz, A. K. (2014). Synthesis and characterization of screen printed Znu thick film for semiconductor device applications. *Physics Research International 2014*. https://doi.org/10.1155/2014/464809 .

Zheng, X., Wang, R., Liddle, B., Wen, Y., Lin, L. and Wang, L. (2022). Crude oil footprint in the rapidly changing world and implications from their income and price elasticities. *Energy Policy 169*, 113204. https://doi.org/10.1016/j.enpol.2022.113204 .